The Limits of Implantable Bluetooth Links in DIY Gel Phantoms: A Channel Gain Evaluation

Mahmoud Wagih, *Member, IEEE* and Nikolas Bruce
James Watt School of Engineering, University of Glasgow, Glasgow, G12 8QQ, U.K.. (Mahmoud.Wagih@glasgow.ac.uk)

***Abstract*—Despite the extensive research in implantable antennas, there are limited reports of practical biotelemetry links or the effects of the channel on in-body communication in ISM-bands. We present a detailed evaluation of an in-body/off-body link using a lossy phantom, showing for the first time the effects of the human body beyond phantom-based studies. A 2.4 GHz patch antenna, with a peak measured gain around −25 dBi, is used in the investigation. A gel phantom is developed using water, sugar, salt, and agar as a binding agent, which can be shaped using 3D-printed moulds. The antenna's reflection coefficient is matched around 2.4 GHz in both the DIY phantom and pork mince, indicating their similarity. Through channel gain measurements, using a VNA and the RSSI of Bluetooth Low Energy (BLE) transceivers, we show that the apparent gain of the implantable antenna can be up to 10 dB lower than its peak gain. A 5.5 m Bluetooth link is demonstrated showing around 15 dB variation in the apparent gain, measured through the RSSI.**

I. Introduction

Body-centric wearable and implantable links are the "interconnect" of future user-centric healthcare monitoring [1], [2]. Nevertheless, it is widely recognised that implantable antennas operate in the most electromagnetically challenging environment [3], [4].

Characterizing implantable antennas, experimentally, in a practical environment is a significant challenge. For instance, despite the extensive research efforts in designing implantable antennas [4], only one study to date has presented measurements in a post-mortem subject [5]. Moreover, such body-scale trials are typically limited to reflection coefficient measurements, and do not explore the far-field performance. *In-vivo*-like measurements in the far-field were carried out in a post-mortem pig [6], but were limited to stationary measurements.

Several low-cost and Do It Yourself (DIY) phantoms have been proposed based on abundant materials [7], [8] and simple processing [9], to enable implantable antennas to be characterized for biotelemetry and wireless power transfer applications. Nevertheless, these phantoms are typically limited in size and are only used in compact demonstrations and not at a full-body scale. Although detailed numerical body models are openly available [10] and can be used to evaluate the near- and far-field antenna properties showing good agreement with measurements [11], they are generally computationally intensive. Moreover, they do not allow the effects of the real-world operation environment, e.g. multi-paths propagation and angular misalignment, to be studied. Thus, there is a clear need for an approach where phantoms can be used to test implantable antennas in their operation environment.

In this paper, we propose a simple low-cost gel DIY phantom, and present the first far-field evaluation of an implantable antenna using a phantom in conjunction with the human body. The antenna design and characterization in both gel and pork mince phantoms are presented in Section II, with the far-field evaluation using lab-grade and real-world setups in Section III.

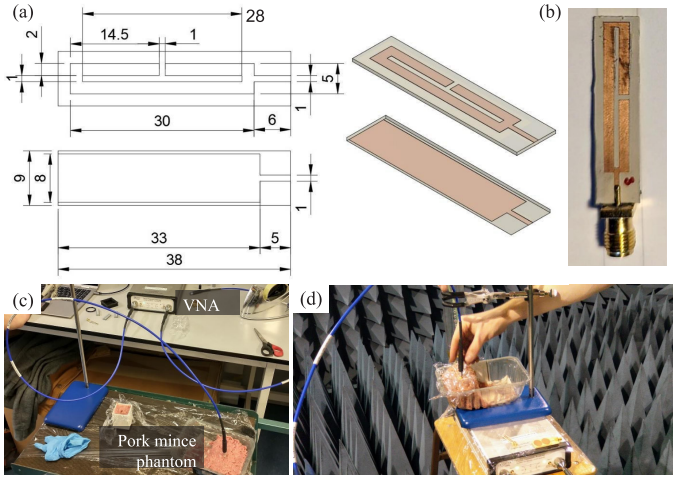

Fig. 1. The microstrip patch antenna used in this work: (a) layout and dimensions (in mm); (b) photograph of the connectorized prototype; (c) *in-vitro* reflection coefficient in a pork mince-based phantom; (d) gain measurements in the anechoic chamber.

II. Antenna and Phantom Design and Evaluation

A. Antenna and Phantom Design

The antenna design used in this work is based on a slotted microstrip patch. The patch is designed on a high-permittivity Rogers RO3010 substrate with ϵ_r=10 and tanδ <0.006. The length of the slot is used to control the input impedance of the antenna for matching in the tissue. Fig. 1(a) and (b) show the layout and photograph, respectively, of the antenna. While the chosen design is larger than state-of-the-art 2.4 GHz implantable antennas [4], the large size allows a reliable connection to be made to the antenna, facilitating measurements, and is in line with previous works where relatively large patch antennas were used for evaluating in-body links [3].

The proposed phantom formulation is based on readily available materials: water, sugar, salt, and, as a bind agent, agar. The ratio of the water, sugar, and salt content is based on the detailed analysis in [9] for liquid phantom. Considering agar is a low permittivity dielectric, the ratio of the agar in the mixture can be adjusted based on the desired firmness, and incorporated in the sugar's mass ratio, based on the formulation in [9]. The mixture used at 2.4 GHz uses approximately 50% sugar (by weight), and under 5% salt to emulate the conductivity of the body. The prepared mixture was heated

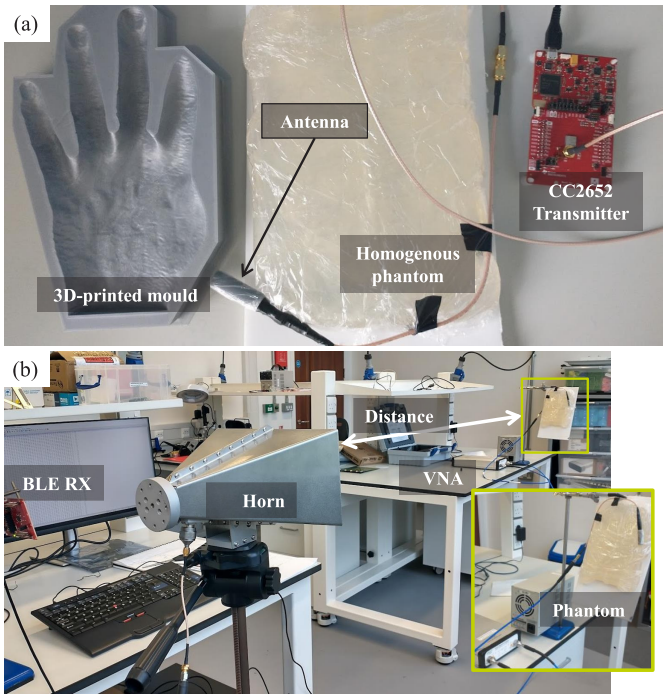

Fig. 2. Measurement setup of the patch antenna in the gel phantom using a Bluetooth transceiver: (a) the encapsulated antenna, phantom, and connected transceiver; (b) far-field measurement setup in an echoic indoor environment.

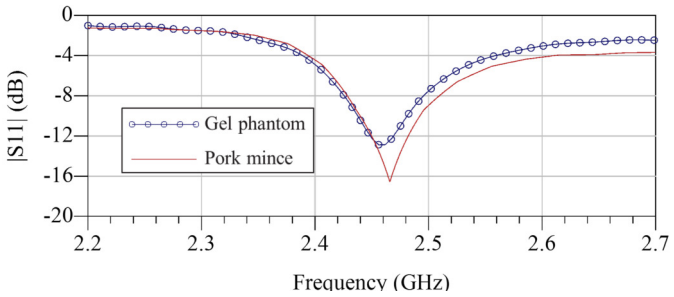

Fig. 3. Measured reflection coefficient of the antenna in the pork mince phantom and the proposed gel phantom.

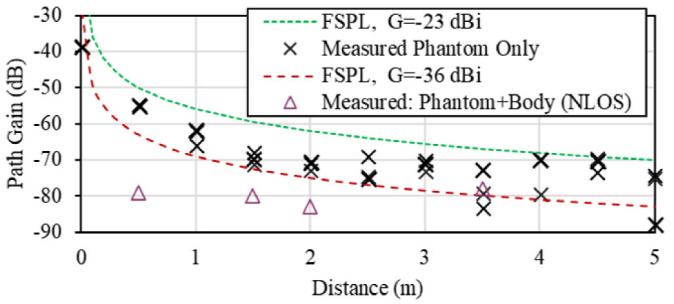

Fig. 4. Measured path gain, using the VNA, between the horn antenna and the implantable antenna in the phantom.

using a hotplate set to 120°C for 8 minutes. Once the solid components have all dissolved, the mixture was allowed to cool down then cast into its mould and set for at least 4 hours. Fig. 2(a) shows the photograph of a hand-shaped 3D-printed mould and a uniform rectangular block used to emulate a human torso section.

B. Antenna Measurements

To validate the antenna's performance in the proposed gel phantom, the antenna's reflection coefficient was measured in a pork mince phantom, pressed to eliminate any air gaps, as shown in Fig 1(c). A PicoVNA6 Vector Network Analyzer (VNA) was used to measure the s-parameters of the antenna. Fig. 3 compares the the reflection coefficient of the antenna in the pork mince to that in the set gel phantom, where a close agreement is observed. In both setups, the antenna is encapsulated using a cylindrical 3D-printed capsule, emulating a packaged implantable device.

In addition to the reflection coefficient measurements, the gain of the implantable antenna was measured in the setup shown in Fig. 1(d). The gain was measured relative to a wire dipole and found to be 25 dBi $\pm$1 dB, at an approximate depth of 2 cm in the mince phantom. The measured is in line with the gain of previous implantable antennas, operating at the same depth, which ranges between -20 and -30 dBi [4].

III. Channel Gain and Biotelemetry Link

A. VNA-Based Channel Gain Measurements

Following the evaluation of the antenna in a compact phantom, the real-world path gain and link performance were evaluated. The antenna, implanted inside the gel phantom, wave evaluated in the setup shown in Fig. 4(b). The path/channel gain was measured using the VNA and a standard gain horn antenna (from Telonic, with a 7 dBi gain in the 2.4 GHz band), over varying distances. In addition, the channel gain was measured when the phantom-implanted antenna was mounted in contact with a subject's torso, with the subject's body in between the horn and the implant, i.e. non-line-of-sight (NLOS). Thus, this measurement combines the near-field absorption of the tissue, from the phantom, and the greater shadowing effects by the body.

Fig. 4 shows the measured path gain between the horn and the implant. For the phantom-only measurements, three points were taken at approximately the same distance, by repositioning the horn for each measurement to capture the randomness introduced by the multi-path propagation. The free-space path loss (FSPL) was calculated based on the horn's 7 dBi gain and two gain thresholds for the implantable antenna: -23 dBi and -36 dBi.

As observed in Fig. 4, the apparent gain of the implantable antenna exhibits up to 15 dB variation and is nearly 10 dB lower than the measured peak gain of approximately 25 dBi. Moreover, the significant randomness in the results shows that the FSPL model, often used in rapidly evaluating biotelemetry margins [12], should not be used to describe the behaviour of implantable antennas in their operation environment.

On the other hand, in NLOS conditions, i.e. when the user's body is blocking the direct propagation path, the channel gain is consistently under -78 dB for a 0.5 m distance between the horn and the implant. This is attributed to the significant absorption of the radiated power through the body, which

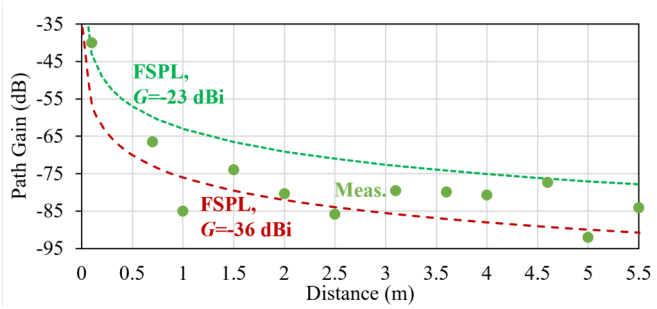

Fig. 5. Measured Bluetooth RSSI over distance, in the same setup as the horn measurements, using the inverted-F antenna on the CC2652RSIP development board as a receiving antenna.

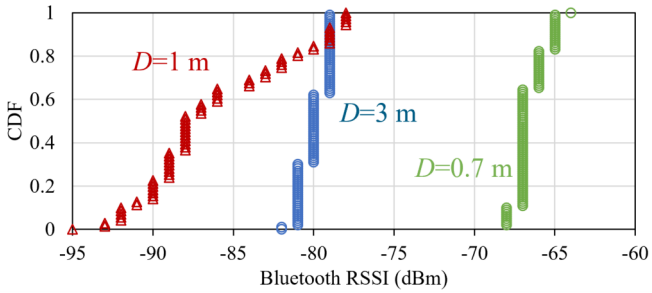

Fig. 6. CDF of the Bluetooth RSSI at different distances between the phantom-implanted antenna the receiver.

fills most of the 50 cm propagation path. However, at further separations, it can be observed that the multi-path reflections improve the transmission in spite of the body shadowing, compared to the 0.5 m case.

B. Bluetooth Low Energy Biotelemetry

The phantom-implanted antenna was connected to a Bluetooth Low Energy (BLE) transceiver (Texas Instruments CC2652RSIP), as shown in Fig. 2(a). Instead of using a horn antenna as a receiver, the inverted-F antenna built into the receiving development board was used. The PCB inverted-F represents a more practical antenna commonly found in a BLE gateway or a phone, and is assumed to have an omnidirectional gain of 2 dBi, based on the manufacturer's datasheet. The received signal strength indicator (RSSI) was used to evaluate the channel gain observed in the more realistic link.

Fig. 5 shows the measured path gain based on the BLE RSSI. The FSPL is also shown for an implant gain of -23 dBi and -36 dBi. While the observed trend is similar to that of the horn-based measurements, significant "dark spots" are observed, e.g. at 1 and 5 m distances. This is likely attributed to the omnidirectionality of the inverted-F antenna, creating more indirect paths and increasing the (destructive) interference between the different arriving signals at the receiver.

To explore the variability in the RSSI, 100 BLE packets were transmitted at each point. The cumulative distribution function (CDF) of the RSSI at different distances is shown in Fig. 6. While limited ± 1 dB variations are observed at intermediate points, i.e. D=0.7 m and D=3 m, significant variation is observed in at the D=1 m point, where an unexpectedly low RSSI was observed. As this dark spot is caused by multi-path interference, the time-variant RSSI will be highly sensitive to slight changes in its operation environment

IV. Conclusions

We presented a new approach to evaluating implantable antennas using gel phantoms in conjunction with living subjects, to allow the channel gain of implantable antennas to be rapidly evaluated. It is shown that the apparent gain of the antenna can be, on average, 10 dB lower than the measured peak gain of the antenna, when evaluated in an echoic environment where multi-path propagation is dominant. The proposed phantom can be rapidly and inexpensively prototyped using salt, sugar, and agar. Our channel gain measurements, using both a VNA and Bluetooth transceiver's RSSI, indicate that biotelemetry limits and performance should be characterized experimentally, or using more practical gain models which account for the random variations in the channel.

References

[1] M. Wagih, L. Balocchi *et al.*, "Microwave-enabled wearables: Underpinning technologies, integration platforms, and next-generation roadmap," *IEEE Journal of Microwaves*, vol. 3, no. 1, pp. 193–226, 2023.

[2] A. Costanzo, F. Benassi, and G. Monti, "Wearable, Energy-Autonomous RF Microwave Systems: Chipless and Energy-Harvesting-Based Wireless Systems for Low-Power, Low-Cost Localization and Sensing," *IEEE Microwave Magazine*, vol. 23, no. 3, pp. 24–38, 2022.

[3] J. Blauert and A. Kiourti, "Bio-matched horn: A novel 1–9 ghz on-body antenna for low-loss biomedical telemetry with implants," *IEEE Transactions on Antennas and Propagation*, vol. 67, no. 8, pp. 5054–5062, 2019.

[4] N. A. Malik, P. Sant *et al.*, "Implantable antennas for bio-medical applications," *IEEE Journal of Electromagnetics, RF and Microwaves in Medicine and Biology*, vol. 5, no. 1, pp. 84–96, 2021.

[5] J. Blauert, Y.-S. Kang, and A. Kiourti, "In vivo testing of a miniature 2.4/4.8 ghz implantable antenna in postmortem human subject," *IEEE Antennas and Wireless Propagation Letters*, vol. 17, no. 12, pp. 2334–2338, 2018.

[6] R. B. Green, M. Hays *et al.*, "An anatomical model for the simulation and development of subcutaneous implantable wireless devices," *IEEE Transactions on Antennas and Propagation*, vol. 68, no. 10, pp. 7170–7178, 2020.

[7] T. Van Nunen, E. Huismans *et al.*, "Diy electromagnetic phantoms for biomedical wireless power transfer experiments," in *2019 IEEE Wireless Power Transfer Conference (WPTC)*, 2019, pp. 399–404.

[8] T. van Nunen, S. Beumer *et al.*, "Characterization of dielectric properties of 3d printing materials for solid biomedical phantoms," in *2022 Asia-Pacific Microwave Conference (APMC)*, 2022, pp. 919–921.

[9] M. Kanda, M. Ballen *et al.*, "Formulation and characterization of tissue equivalent liquids used for rf densitometry and dosimetry measurements," *IEEE Transactions on Microwave Theory and Techniques*, vol. 52, no. 8, pp. 2046–2056, 2004.

[10] J. W. Massey and A. E. Yilmaz, "Austinman and austinwoman: High-fidelity, anatomical voxel models developed from the vhp color images," in *2016 38th Annual International Conference of the IEEE Engineering in Medicine and Biology Society (EMBC)*, 2016.

[11] M. Wagih, G. S. Hilton *et al.*, "Dual-Polarized Wearable Antenna/Rectenna for Full-Duplex and MIMO Simultaneous Wireless Information and Power Transfer (SWIPT)," *IEEE Open Journal of Antennas and Propagation*, vol. 2, pp. 844–857, 2021.

[12] A. Iqbal, M. Al-Hasan *et al.*, "A compact implantable mimo antenna for high-data-rate biotelemetry applications," *IEEE Transactions on Antennas and Propagation*, vol. 70, no. 1, pp. 631–640, 2022.